



Formation of nitrous oxide over Pt-Pd oxidation catalysts: Secondary emissions by interaction of hydrocarbons and nitric oxide

Patrick Lott^{a,*}, Simon Bastian^a, Heike Többen^b, Lisa Zimmermann^b, Olaf Deutschmann^{a,c}

^a Institute for Chemical Technology and Polymer Chemistry (ITCP), Karlsruhe Institute of Technology (KIT), Engesserstr. 20, 76131 Karlsruhe, Germany

^b Purem GmbH, Eberspächerstr. 24, 73730 Esslingen, Germany

^c Institute of Catalysis Research and Technology (IKFT), Karlsruhe Institute of Technology (KIT), Hermann-von-Helmholtz-Platz 1, 76344 Eggenstein-Leopoldshafen, Germany

ARTICLE INFO

Keywords:

Emission control
HC-deNOx
Nitrous oxide
Pt-Pd catalyst
Secondary emissions

ABSTRACT

The interaction of hydrocarbons (HC) and nitric oxide (NO) over noble metal catalysts for exhaust gas after-treatment of lean-operated combustion engines can lead to secondary emissions, namely the formation of nitrous oxide (N₂O), which is a strong greenhouse gas calling for N₂O reduction concepts. By means of a series of light-off tests over state-of-the-art Pt-Pd oxidation catalysts, this study identifies the most critical catalyst operation regimes that should be avoided in order to minimize N₂O levels. Especially unsaturated HCs react with NO to form significant amounts of N₂O between 150 °C and 350 °C; an increasing HC/NOx ratio generally promotes N₂O formation, whereas the NO oxidation reaction is increasingly inhibited. Since low space velocities and fast catalyst heating allow for minimizing N₂O levels, active heating of catalytic converters during cold start and phases of low exhaust gas temperatures may efficiently reduce the formation of N₂O in real-world applications.

1. Introduction

After decades of research on exhaust gas after-treatment systems, modern catalytic converters ensure an efficient emission abatement for combustion engines running on diesel, gasoline, and natural gas [1–4]. While the first after-treatment systems comprised only a single oxidation catalyst, state-of-the-art exhaust tailpipes combine several converters and technologies to account for conversion of all exhaust gas species and continuously tightening emission legislation calls for even more complex after-treatment systems. In addition to economic considerations, especially the limited space in mobile applications drives the development of innovative compact catalytic converters that possibly merge different technologies in a single device. This compact design results in competitive adsorption on the catalyst surface and promotes interactions of the many different exhaust gas species, which can ultimately lead to the formation of additional pollutants, so-called secondary emissions, such as ammonia (NH₃) [5–7], nitrous oxide (N₂O) [8–10], and even very toxic compounds like hydrogen cyanide (HCN) [11–13]. In contrast to earlier regulations, current and upcoming legislation will introduce very stringent limits for secondary emissions, among which N₂O is considered particularly critical, since it has a more

than 300 times higher global warming potential than that of carbon dioxide (CO₂) and exhibits an ozone depleting effect [14–16].

N₂O is a pollutant that is relevant for all kinds of combustion engine applications [16], as it forms as an undesired byproduct in stoichiometric exhausts over three-way catalysts (TWC) [7,17–19] and in the exhaust tailpipe of lean-burn engines alike [14,20]. In the latter case, especially deNOx-converters for selective catalytic reduction (SCR) of nitrogen oxides (NOx) using ammonia (NH₃) [9,21–23] or hydrocarbons (HCs) [20,24–26] as reducing agent are prone to N₂O evolution. The interaction of nitric oxide (NO) and HCs over noble metal based catalysts was subject to several mechanistic studies aiming at unraveling the complex reaction pathways causing formation of N₂O during deNOx reactions over oxidation catalysts. In short, three different mechanisms are considered: First, surface isocyanate species (R-NCO) were reported as the most relevant intermediates during NOx reduction via HC-SCR, whose reaction with NO ultimately results in N₂O formation [27–29]. Second, organic nitro compounds or derivatives and related species were suggested as most relevant intermediate compounds [30–33], e.g. with N₂O (and ketone) formation from oximes (R₁R₂C=N-OH) [33]. Third, several studies [24,34–37] suggested dissociative NO adsorption on the noble metal surface and subsequent oxygen reduction by

* Corresponding author.

E-mail address: patrick.lott@kit.edu (P. Lott).

<https://doi.org/10.1016/j.apcata.2023.119028>

Received 1 November 2022; Received in revised form 28 December 2022; Accepted 7 January 2023

Available online 10 January 2023

0926-860X/© 2023 The Author(s). Published by Elsevier B.V. This is an open access article under the CC BY license (<http://creativecommons.org/licenses/by/4.0/>).

hydrocarbon species as mechanism for HC-deNO_x, with N₂O forming by a combination of an adsorbed (undissociated) NO molecule and an adsorbed N atom [34,36].

Especially the catalyst operation conditions influence the emerging N₂O levels during HC-SCR over noble metal based catalysts [24,25,38,39], aside from catalyst formulation [35,40] and material-related catalyst properties like noble metal particle size [41], alloying state [42], or sulfation [43] that may change due to degradation, hereby causing changes in the catalytic activity for hydrocarbon, carbon monoxide (CO), and NO_x conversion. Since in the context of HC-SCR the type of hydrocarbon used as reductant plays a particular role, a wide variety of hydrocarbons has been suggested for NO_x removal. Among other species, particularly ethylene (C₂H₄) [35], propylene (C₃H₆) [26,36,44], propane (C₃H₈) [36,40], n-octane (C₈H₁₈) [45], and even aromatic compounds like toluene (C₇H₈) [46] have been tested for HC-SCR, with the latter one being proposed as reductant that avoids N₂O production over noble metal catalysts. In general, unsaturated hydrocarbons are more reactive, which allows for significant HC-NO_x interactions already at comparably low temperatures and an onset of N₂O formation around 130–200 °C, depending on the catalyst formulation [26,35,40,47,48]. In contrast, saturated hydrocarbons with their lower reactivity are typically activated at slightly higher temperatures, which consequently shifts the onset of NO_x-reduction as well [36,40,47]. Moreover, both short-chain species like C₃H₆ as well as long-chain species such as dodecane (C₁₂H₂₆), are known to inhibit NO oxidation to nitrogen dioxide (NO₂) over Pt-Pd oxidation catalysts, since during hydrocarbon oxidation NO₂ is preferentially consumed compared to oxygen (O₂) [49,50]. In contrast, hydrocarbons can also impede an overoxidation of the platinum surface; the consumption of surface oxygen by hydrocarbons can be particularly beneficial for NO oxidation [50] that preferentially takes place over reduced noble metal surface sites [51,52]. These observations are also highly relevant in the context of SCR. As already mentioned above, hydrocarbon and NO conversion rates as well as possible byproduct formation strongly depend on the adsorbed surface species, which in turn are heavily influenced by the gas species concentrations and by the species residence time or in terms of the macroscopic operation conditions the gas hourly space velocity (GHSV), respectively.

A successful suppression of N₂O formation requires both, a detailed knowledge of the formation pathways as well as a profound database on the conditions that support N₂O formation. Hence, our present study revisits the topic of N₂O formation caused by HC-NO_x interactions by a comprehensive measurement campaign that comprises kinetic tests under a wide variety of conditions of two different diesel oxidation catalysts (DOC) that are used for heavy-duty applications and passenger car systems, respectively. Based on our results we consider the effect of hydrocarbon type (unsaturated vs. saturated), temperature, space velocity, and the HC/NO_x ratio as the most relevant factors on N₂O formation. The final objective of this study is to provide guidance for optimization of operating conditions to minimize N₂O emissions.

2. Experimental

2.1. Catalyst materials

Within this study, two different commercial diesel oxidation catalysts purchased from commercial sources served as materials for catalytic testing. Both samples consist of a cordierite substrate (400 cpsi) that is coated with a Pt-Pd washcoat (noble metal ratio 3:1). The first catalyst sample (DOC-1) exhibits a total noble metal loading of 12 g/ft³ (corresponding to approx. 0.42 g/L) and is representative for an after-treatment system used in commercial diesel vehicles for heavy-duty applications, whereas the second catalyst sample (DOC-2) has a substantially higher noble metal loading of 100 g/ft³ (corresponding to approx. 3.53 g/L), which is representative for oxidation catalysts that are used in lean-burn passenger car systems and therefore light-duty

applications. Herewith, we chose two different industrially relevant catalyst systems that were subject to extensive testing under well-defined conditions in a lab-scale catalyst testing bench. Cylindrical lab-size samples with a diameter *d* of 2.54 cm and a length *l* of 5.00 cm were obtained by cutting the full-size commercial catalysts. In order to ensure a stable catalyst during the performance tests, a degreening procedure that consisted of an exposure to 10 vol.-% H₂O in air (60 000 h⁻¹) for 4 h at 700 °C was conducted for both samples prior to these tests.

2.2. Catalyst testing bench

The kinetic data were obtained using a synthetic exhaust gas lab-bench catalyst testing unit that was already described in detail in an earlier study [10]. The setup essentially consists of a furnace-heated quartz glass tubular reactor (plug-flow configuration; inner diameter: 2.54 cm, length: 100 cm) that contains the lab-size catalyst sample (*d* = 2.54 cm, *l* = 5.00 cm). Mass flow controllers and a controlled evaporation mixer precisely dose reaction gases (originating from gas bottles) and steam (from a pressurized water tank). The only liquid hydrocarbon used in this study, C₁₂H₂₆, is dosed by bubbling nitrogen (N₂) gas through a heated stainless-steel tank filled with C₁₂H₂₆; herein, the C₁₂H₂₆ concentration is controlled by varying the inert N₂ flow and the temperature of the tank. Two type N thermocouples approx. 2 mm up- and downstream the sample are used to control and monitor the inlet and outlet temperatures and a Fourier-transform infrared (FTIR) spectrometer (MG2030, MKS Instruments) continuously analyzes the effluent reaction gas stream.

2.3. Testing conditions and procedure

The experimental testing matrix comprises a systematic variation of the gas composition, the gas hourly space velocity (GHSV), and the reaction temperature at ambient pressure. A typical exhaust gas mixture relevant for lean-burn applications was used, excluding CO₂ that is considered playing a subordinate role [49], but including the unavoidable exhaust gas component water (H₂O), which is known as a potential inhibitor due to a blockage of noble metal surface sites [53,54]. In addition to a base gas feed of 150 ppm NO, 10 vol.-% O₂, 10 vol.-% H₂O and balance N₂, a HC concentration of 150 ppm, 375 ppm, 750 ppm, 1500 ppm or 7500 ppm was added, which corresponds to a HC/NO_x ratio of 1.0, 2.5, 5.0, 10.0, and 50.0, respectively (molar concentrations). Considering dynamic operation conditions of real-world applications, particularly in the mobility sector, these HC/NO_x ratios replicate an industrially relevant range of conditions that can occur during engine operation. In order to cover different types of hydrocarbons that can be present in exhaust gases – saturated and unsaturated species, long-chain versus short-chain HCs – tests were performed using either C₂H₄, C₂H₆, C₃H₆, C₃H₈, or C₁₂H₂₆; note that only one hydrocarbon was dosed at a time. Table 1 summarizes the gas composition variation. Using C₂H₄ as model compound, GHSV values of 30 000 h⁻¹, 60 000 h⁻¹, and 90 000 h⁻¹ were chosen to uncover the influence of the space velocity on N₂O formation. Performing light-off runs with a temperature ramp of 5 °C/min and 15 °C/min, respectively, provides

Table 1
Gas matrix of the experimental measurement campaign.

Mix ^a	NO / ppm	HC / ppm	O ₂ / vol.-%	H ₂ O / vol.-%	N ₂	HC/NO _x
Xa	150	150	10	10	balance	1.0
Xb	150	375	10	10	balance	2.5
Xc	150	750	10	10	balance	5.0
Xd	150	1500	10	10	balance	10.0
Xe	150	7500	10	10	balance	50.0

^a The X represents a number that identifies the hydrocarbon used during the kinetic test, with 1 = C₂H₄, 2 = C₂H₆, 3 = C₃H₆, 4 = C₃H₈, and 5 = C₁₂H₂₆.

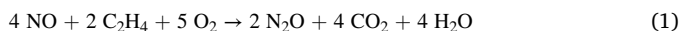
information on temperature and ramp rate effects.

3. Results and discussion

3.1. Temperature-dependent evolution of gas species

Fig. 1 shows the temperature-dependent conversion and species concentration trends as obtained during a light-off test in 150 ppm NO, 750 ppm C₂H₄, 10 vol.-% O₂, 10 vol.-% H₂O, bal. N₂ (gas mix 1c, 5 °C/min, GHSV = 60 000 h⁻¹). In line with earlier research [35], the simultaneous dosage of NO and C₂H₄ in a lean gas mixture results in considerable N₂O formation. Under the conditions chosen, the N₂O concentration reaches a maximum of 48 ppm at 190 °C over DOC-1 and 57 ppm at 166 °C over DOC-2, respectively. Overall, DOC-2 exhibits a higher oxidation activity, both for NO and C₂H₄, which does not only result in higher N₂O concentrations but also seems to broaden the temperature window in which N₂O is formed. Regarding the trends of the gas phase species concentrations, the onset of C₂H₄ and NO conversion gives rise to the N₂O signal. Notably, N₂O formation is favored over NO₂ formation below ~225 °C and the maximum N₂O concentration is detected at the maximum NO conversion and once the catalyst fully converts C₂H₄. A further temperature increase during the light-off test results in a continuous shift of the product selectivity from N₂O to NO₂, which goes along with an overall declining NO conversion over both catalyst samples. Notably, the NO conversion is less than 60% over DOC-1 in the temperature window between 250 °C and 350 °C, whereas the NO conversion decreases from about 80% at 250 °C to approximately 62% at 350 °C over DOC-2. Simultaneously, the N₂O level drops substantially and only 1 ppm and ~1.7 ppm N₂O are found over DOC-1 and DOC-2, respectively, at the maximum temperature of 350 °C. Note, that no NH₃ formation was observed during the light-off tests.

From a mechanistic point of view, N₂O evolves as a byproduct of NOx reduction by C₂H₄ [25], with the global reaction Eqs. (1) and (2) being possible N₂O formation pathways:



Hence, the simultaneous activation of both C₂H₄ and NO is a prerequisite not only for the SCR of NO to N₂, which would typically be desired in the context of NOx removal, but also for N₂O formation, which explains the correlation of the NO and C₂H₄ conversion curves with the N₂O concentration curve in Fig. 1. In this respect, varying hydrocarbon inlet concentrations have an impact on both the temperature evolution due to the exothermicity of C₂H₄ oxidation as well as the surface chemistry taking place on the noble metal. These aspects are discussed in detail in the following Section 3.2.

3.2. Influence of C₂H₄/NOx ratio

The data shown in Fig. 2 illustrate that the N₂O emission profiles strongly depend on the C₂H₄/NOx ratio. In particular, increasing C₂H₄/NOx ratios promote N₂O formation over a broad temperature range (Fig. 2a, b) and substantially increase the maximum N₂O concentration ($c(\text{N}_2\text{O})_{\text{max}}$). At the same time, $T(c(\text{N}_2\text{O})_{\text{max}})$, which is the temperature where the maximum N₂O concentration is observed, drops over both catalysts (Fig. 2c, d). Herein, $T(c(\text{N}_2\text{O})_{\text{max}})$ is the gas temperature measured at the catalyst inlet and therefore remains unaffected by the exothermicity of the hydrocarbon oxidation. However, the exothermicity could be one reason for the drop of $T(c(\text{N}_2\text{O})_{\text{max}})$ with increasing C₂H₄/NOx ratios: As illustrated in Fig. 2e and f that shows the C₂H₄ conversion as well as the difference between the catalyst's inlet and outlet temperature, ΔT , as a function of the (inlet) temperature, higher C₂H₄ concentrations give rise to pronounced temperature gradients along the catalyst samples. Since especially at elevated temperatures typically not the entire length of the catalyst sample is needed for full hydrocarbon conversion [49], temperature zones within the monolithic catalyst will arise, i.e. a particularly hot zone in the front part where C₂H₄ is converted, that may benefit N₂O formation. When exposing DOC-1 to a light-off test in gas mix 1d, for instance, the inlet gas stream temperature $T(c(\text{N}_2\text{O})_{\text{max}})$ is 183 °C whereas the outlet temperature is 219 °C, hence yielding a ΔT of 36 °C. Increasing the C₂H₄ concentration even further to a C₂H₄/NOx ratio of 50 results in pronounced heat formation, i.e. for DOC-1 an inlet temperature of 200 °C corresponds to an outlet temperature of 489 °C, that allows to mostly skip the critical temperature for the most part of the monolith length (Fig. 2e, f; purple line). Consequently, the N₂O concentration instantly drops after reaching its maximum $c(\text{N}_2\text{O})_{\text{max}} = 37$ ppm at 170 °C and at inlet temperatures below 180 °C N₂O formation is negligible due to the high exothermicity. These results indicate that higher ramp rates allow passing critical temperature windows faster and, as extensively discussed in Section 3.3, contribute to minimizing N₂O formation.

Since both our kinetic tests and previously reported mechanistic insights [20,29] suggest a strong contribution of the hydrocarbon concentration on N₂O formation during HC-deNOx, we tried to correlate the C₂H₄ conversion, the maximum N₂O concentration ($c(\text{N}_2\text{O})_{\text{max}}$), and the corresponding temperature $T(c(\text{N}_2\text{O})_{\text{max}})$. Under the conditions chosen for the light-off tests displayed in Fig. 2 with a ramp rate of 5 °C/min, C₂H₄ was almost fully converted at $T(c(\text{N}_2\text{O})_{\text{max}})$ for all C₂H₄ inlet concentrations over DOC-2. In contrast, full C₂H₄ conversion was not always reached at $T(c(\text{N}_2\text{O})_{\text{max}})$ during the tests with a ramp rate of 15 °C/min (Fig. S1c-f). For instance, during the test with DOC-2 in gas mixture 1d (C₂H₄/NOx ratio = 10, $T_{\text{ramp}} = 15$ °C/min), a maximum N₂O concentration of 68 ppm and a C₂H₄ conversion of 94% was observed at $T(c(\text{N}_2\text{O})_{\text{max}}) = 162$ °C (Fig. S2). Under identical conditions, DOC-1,

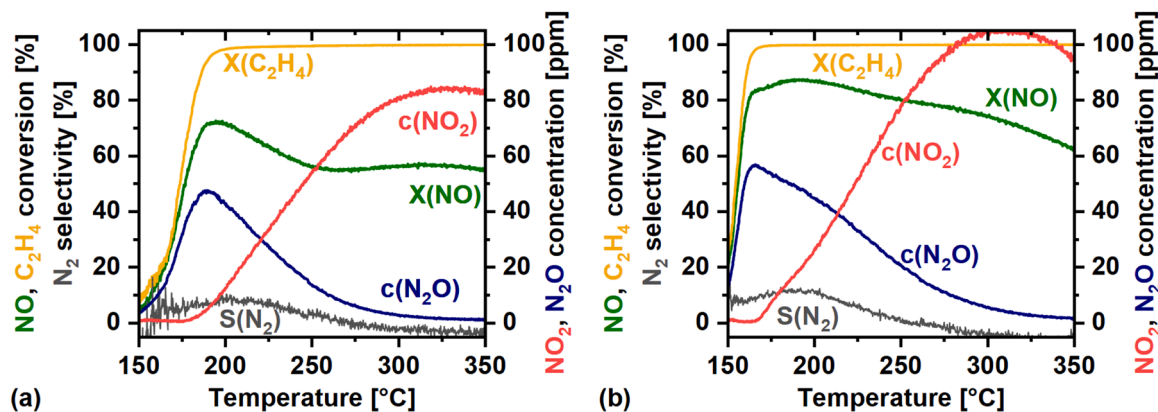


Fig. 1. Conversion of NO and C₂H₄, N₂ selectivity, and the concentrations of NO₂ and N₂O during a light-off in 150 ppm NO, 750 ppm C₂H₄, 10 vol.-% O₂, 10 vol.-% H₂O, bal. N₂ (gas mix 1c, 5 °C/min, GHSV = 60 000 h⁻¹) over (a) DOC-1 and (b) DOC-2.

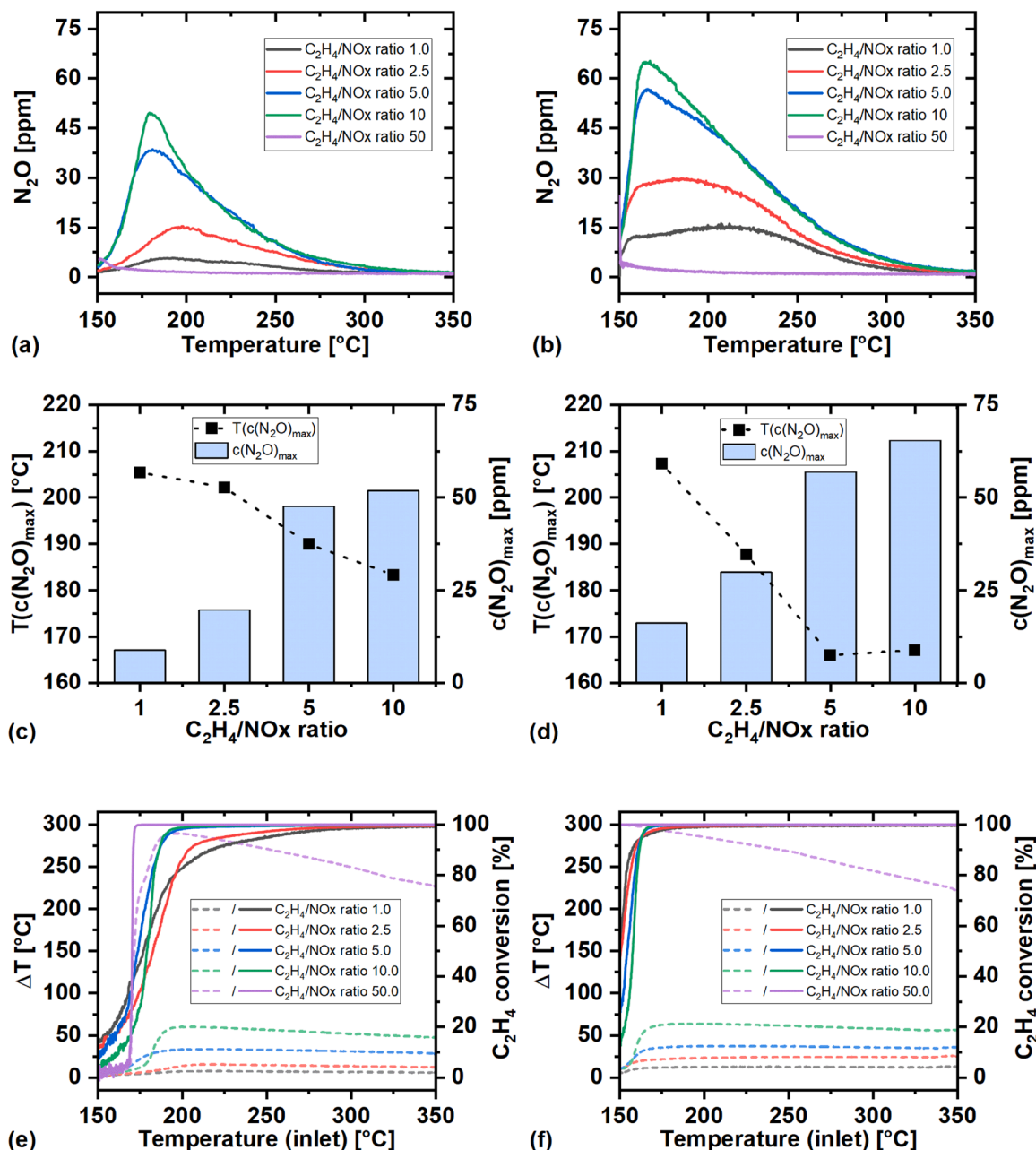


Fig. 2. N_2O evolution during a light-off in 150 ppm NO, 150 – 7500 ppm C_2H_4 , 10 vol.-% O_2 , 10 vol.-% H_2O , bal. N_2 ($5^\circ\text{C}/\text{min}$, GHSV = $60\,000\ \text{h}^{-1}$) over (a) DOC-1 and (b) DOC-2, the maximum N_2O concentration $c(\text{N}_2\text{O})_{\text{max}}$ with the corresponding temperature $T(c(\text{N}_2\text{O})_{\text{max}})$ for (c) DOC-1 and (d) DOC-2, and the C_2H_4 conversion (solid lines) as well as the difference between the inlet and outlet temperature of the catalyst, ΔT (dashed lines), versus the (inlet) temperature for (e) DOC-1 and (f) DOC-2.

which exhibits a generally lower catalytic activity that can be attributed to its lower noble metal loading, achieved only 77% C_2H_4 conversion at $T(c(\text{N}_2\text{O})_{\text{max}}) = 179^\circ\text{C}$, while producing 50 ppm N_2O (Fig. S2). Furthermore, the overall trends depicted in Fig. 2d (as well as in Fig. S1d for a ramp rate of $15^\circ\text{C}/\text{min}$) point to a minimum $T(c(\text{N}_2\text{O})_{\text{max}})$ of approximately 165°C ($\pm 3^\circ\text{C}$). In particular, an increase of the $\text{C}_2\text{H}_4/\text{NOx}$ ratio from 5.0 to 10.0 over DOC-2 does not result in a drop in $T(c(\text{N}_2\text{O})_{\text{max}})$ (Fig. 2d) as observed for DOC-1 (Fig. 2c). Under consideration of the more pronounced heat evolution that occurs when the hydrocarbon concentration increases (Fig. 2e, f for light-off tests with a ramp rate of $5^\circ\text{C}/\text{min}$ and Fig. S1e, f for those with $15^\circ\text{C}/\text{min}$), our data do not suggest a simple direct correlation between the hydrocarbon conversion and the maximum N_2O formation rate, but rather point to a more complex interplay of different phenomena. On the one hand,

temperature effects that are influenced by the exothermicity and consequently depend on the hydrocarbon concentration are particularly relevant in the low-temperature regime, since during the light-off already minor changes of the temperature can have a strong impact on the conversion of the hydrocarbon. On the other hand, with increasing temperature also the oxidation of NO to NO_2 comes into play, which is subject of the following paragraph.

Regarding the NO conversion profiles, which are plotted in Fig. 3a for DOC-2, a transition regime between 250°C and 300°C is observed where the conversion curves intersect. At temperatures below 250°C , an increasing C_2H_4 inlet concentration promotes NO removal, which is exemplarily illustrated in the top part of Fig. 3b at 200°C . Irrespective of the HC/NOx ratio, the NO conversion rises to a maximum and drops continuously afterwards (Fig. 3a). On the other hand, high C_2H_4

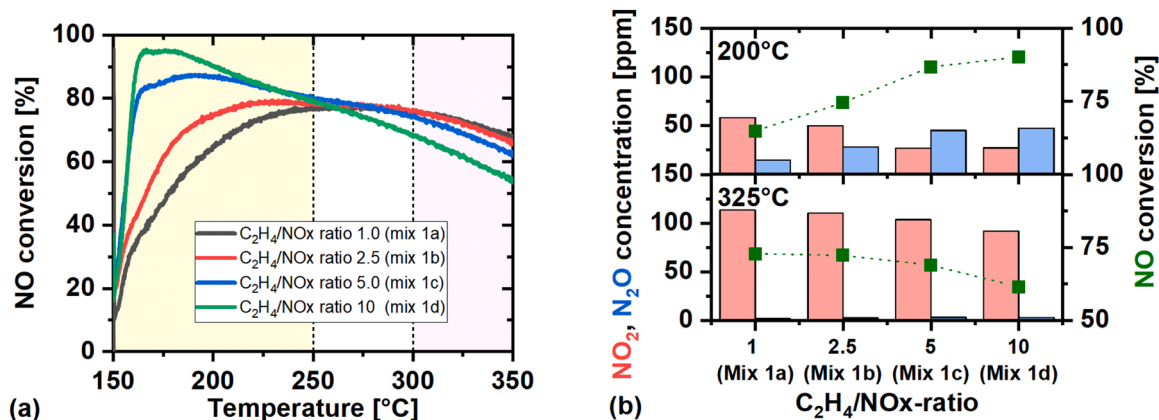


Fig. 3. (a) NO conversion during a light-off in 150 ppm NO, 150 – 750 ppm C₂H₄, 10 vol.-% O₂, 10 vol.-% H₂O, bal. N₂ (5 °C/min, GHSV = 60 000 h⁻¹) over DOC-2. (b) NO₂ and N₂O concentration as well as NO conversion as function of the C₂H₄/NO_x ratio during the light-off tests at 200 °C (top) and 325 °C (bottom).

concentrations inhibit NO conversion above 300 °C; the bottom part of Fig. 3b underscores this declining NO conversion at 325 °C with rising C₂H₄/NO_x ratios, which is an inverted trend compared to the low-temperature regime. Taking the species evolution analogous to those shown in Fig. 1 into account, we can conclude that at low temperatures the catalytic HC-SCR reactions dominate the NO_x profiles. In contrast, the NO oxidation becomes the dominant catalytic process at higher temperatures, with NO₂ as the main reaction product (Fig. S3). Based on spatially resolved species concentration profiles obtained by Irani et al. [49], we can expect that above 300 °C the major share of hydrocarbons is converted in the front half of the monolith. Nevertheless, the remaining amount of hydrocarbons that are still present in the second half and whose conversion may require most or even the entire length of the monolith is sufficient to inhibit NO oxidation [49,50], which explains the trend reversal regarding the hydrocarbon concentration impact on the NO_x conversion depicted in Fig. 3a and the decreasing overall NO₂ concentrations that can be observed at higher temperatures, e.g. as exemplarily shown in Fig. 3b for 325 °C.

In summary, the results discussed above suggest that N₂O evolution can be circumvented twofold: Either the hydrocarbon concentration is kept as low as possible, simply resulting in a shortage of HC-species that could interact with NO, which consequently minimizes N₂O formation, or the hydrocarbon concentration is kept so high that the exothermicity generated by the total oxidation of C₂H₄ provides sufficient thermal energy to heat the catalyst beyond the critical temperature range. In the latter case, the low NO to NO₂ oxidation needs to be considered, which does not only originate from an inhibition due to the presence of C₂H₄, but which also occurs due to the thermodynamic NO-NO₂ equilibrium that is increasingly shifted toward NO with rising temperature despite the presence of excess oxygen [55].

3.3. Influence of space velocity

Since an increase of the space velocity results in faster passage of reactive gases through the monolith and reduces the time of pollutant-catalyst interaction, the hydrocarbon conversion and consequently also the N₂O selectivity are shifted to higher temperatures (Fig. S4). During a light-off with DOC-2 in 150 ppm NO, 750 ppm C₂H₄, 10 vol.-% O₂, 10 vol.-% H₂O, bal. N₂, for instance, T₉₀(C₂H₄) increases from 153 °C at 30 000 h⁻¹ to 171 °C at 90 000 h⁻¹. Similarly, an increasing GHSV shifts the maximum N₂O selectivity towards higher temperatures. Although beyond the simple shift in temperature both the selectivity profiles and the absolute N₂O concentrations essentially remain unchanged, the total amount of N₂O that is formed during the light-off test substantially increases with increasing space velocity, irrespective of the catalyst sample. Obviously, the activity of the catalyst is sufficient to activate all C₂H₄ and NO molecules not only at low space velocity (30

000 h⁻¹) but also at high space velocity (90 000 h⁻¹), hence, despite a constant molar fraction of NO in the inlet gas flow, the total amount of NO converted to N₂O varies with the space velocity. In order to allow for a direct comparison, the N₂O amount in milligram (mg) produced per catalyst volume in liter (L) during each light-off test was calculated using the N₂O signal versus time; further details can be found in the Fig. S1.

Fig. 4 summarizes the N₂O production for both catalyst samples that were operated at different space velocities, C₂H₄/NO_x ratios, and with different temperature ramps during the light-off. The comparison of the subfigures a-d of Fig. 4 reveals some general trends that are valid for both catalyst samples. In addition to the already discussed higher total N₂O amounts formed during catalytic tests at higher GHSV, the data clearly demonstrate that the N₂O evolution strongly correlates with the HC/NO_x ratio: the higher the hydrocarbon concentration in the inlet gas flow, the higher is the N₂O production. This trend is valid up to a C₂H₄/NO_x ratio of 5 over DOC-1 and of 10 over DOC-2, respectively. However, the N₂O amount formed drops significantly when using a ratio of 50, for instance when comparing the light-off with 5 °C/min and a GHSV of 60 000 h⁻¹ using mix 1d and mix 1e by a factor of approximately 4 over DOC-1 and by a factor of almost 10 over DOC-2. This behavior is due to the pronounced heat evolution when exposing the catalyst to high hydrocarbon amounts, namely 1500 ppm C₂H₄ for mix 1d versus 7500 ppm C₂H₄ for mix 1e, which mostly avoids the presence of critical temperature regimes along the catalyst sample that would allow for N₂O evolution. Notably, the more active sample DOC-2 oxidizes C₂H₄ at even lower temperatures, hereby passing the critical temperature regime that allows for N₂O formation even faster. If operated at 30 000 h⁻¹, both samples tested are capable of fully converting 7500 ppm C₂H₄ at inlet temperatures as low as 150 °C. The absence of an N₂O signal for these light-off tests suggests that under these conditions the high exothermicity enables the hydrocarbon conversion taking place so fast that the HC-NO_x interactions that could result in N₂O formation are suppressed.

While the N₂O concentration curves remain mostly unchanged when varying the heating ramp (Fig. 2 and Fig. S1), the comparison of the total N₂O amounts formed during the light-off tests reveals a striking reduction of the N₂O quantity when choosing higher ramp rates. Notably, a faster passage of the critical temperature window, e.g. when using 15 °C/min (Fig. 4c, d) instead of 5 °C/min (Fig. 4a, b), is the most efficient measure to reduce the overall N₂O formation over the catalyst. Regarding real-world applications, this corresponds to engine operation phases with high loads that contribute to passing the critical temperature range as fast as possible. In addition, active heating of the exhaust tailpipe may be a suitable approach to circumvent longer periods of temperature regimes enabling N₂O formation.

In terms of total N₂O amounts formed during the light-off tests, the effect of catalyst loading on N₂O formation is most pronounced at a C₂H₄/NO_x ratio of 1.0 and seems to reduce with rising hydrocarbon

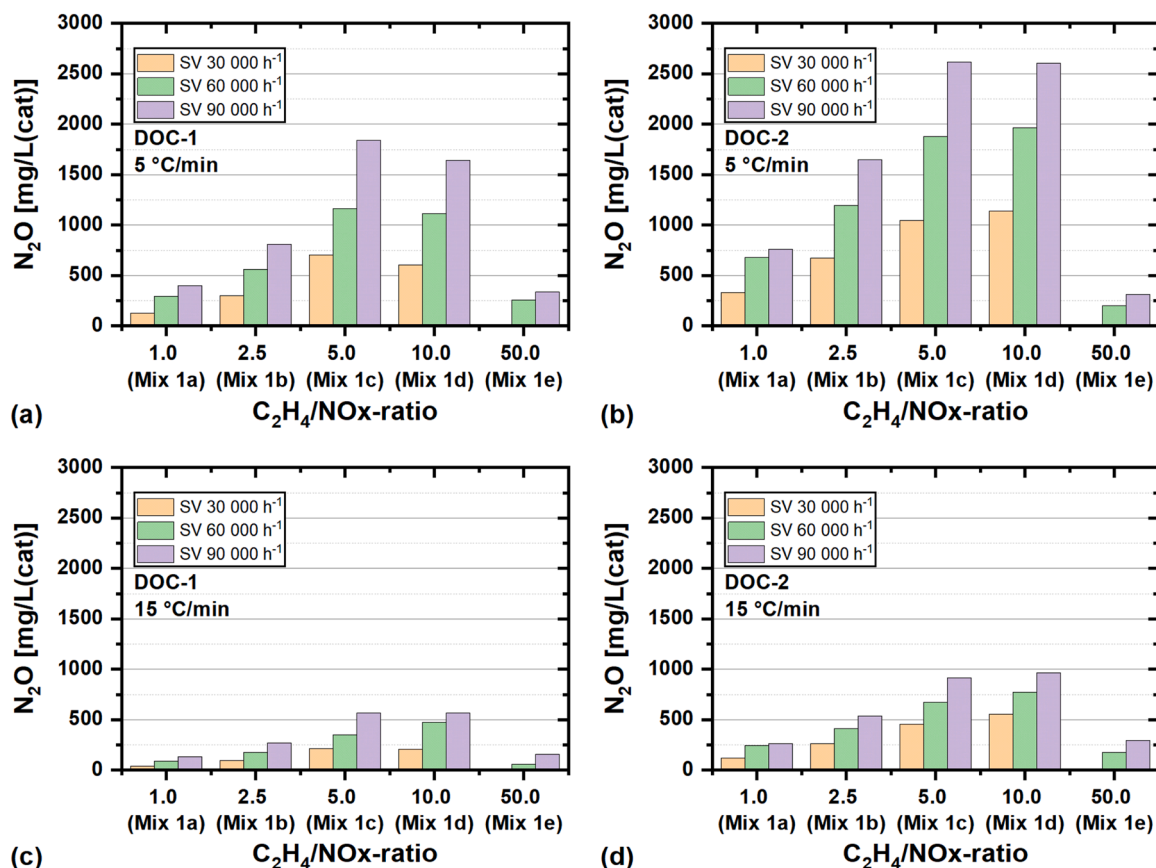


Fig. 4. Total amount of N_2O formed during a light-off from 150° to 350°C in 150 ppm NO, 150 – 7500 ppm C_2H_4 , 10 vol.-% O_2 , 10 vol.-% H_2O , bal. N_2 (GHSV = 30 000, 60 000, 90 000 h^{-1}) over DOC-1 (a, c) and DOC-2 (b, d); ramp rate 5 °C/min (a, b) and 15 °C/min (c, d), respectively.

concentrations. For instance, the light-off for DOC-2 in gas mix 1a using a space velocity of 60 000 h^{-1} and a ramp rate of 5 °C/min yields about 680 mg(N_2O)/L(cat) and consequently produces a 2.3 times larger quantity than DOC-1 with only 295 mg(N_2O)/L(cat) under identical conditions. In contrast, this factor drops to about 1.7 in gas mix 1d. The different behavior of the two catalyst samples becomes even clearer when plotting the N_2O amount formed during a single light-off in relation to the total amount of NO dosed during the light-off as depicted in Fig. 5. Within the accuracy of the data, changes of the space velocity do not cause major changes of the NO to N_2O conversion over DOC-1

(Fig. 5a). In contrast, related to the NO amount dosed during a light-off test, a more pronounced N_2O evolution is found over DOC-2 with decreasing space velocity (Fig. 5b).

While the very different noble metal loading, namely 12 g/ft³ for DOC-1 and 100 g/ft³ for DOC-2, can clearly be identified as reason for the different behavior of the two systems, we can only speculate about the microkinetic and microscopic reasons at this point. These comprise a different surface site availability for adsorption and reaction that is presumably higher over DOC-2, differences in the noble particle size that have a direct impact on the redox-behavior of the catalysts, and

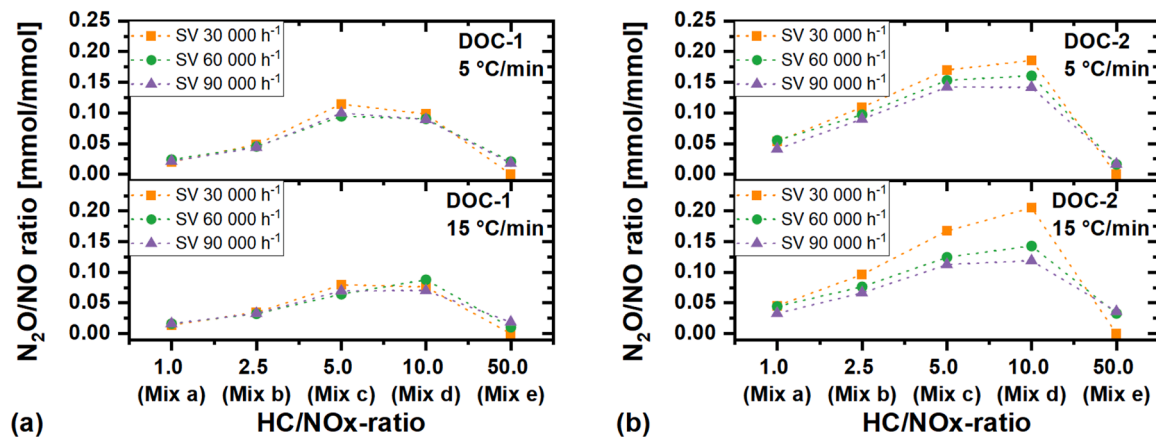


Fig. 5. N_2O amount formed (in mmol) in relation to the NO amount dosed (in mmol) during each light-off test from 150° to 350°C in 150 ppm NO, 150 – 7500 ppm C_2H_4 , 10 vol.-% O_2 , 10 vol.-% H_2O , bal. N_2 (GHSV = 30 000, 60 000, 90 000 h^{-1}) with a temperature ramp rate of either 5 °C/min (top) or 15 °C/min (bottom) as a function of the HC/NOx ratio for (a) DOC-1 and (b) DOC-2.

diffusion limitations in the washcoat. In fact, contradictory findings have been reported on the role of the particle size on the selectivity and activity and thereby related phenomena like competition for surface sites and redox-behavior, and their exact role is at least partly still under debate in the context of HC-SCR [39,56–58]. While the higher noble metal loading of DOC-2 clearly promotes the activation of NO and C₂H₄ already at low temperatures (Fig. 1) and causes an overall higher N₂O production compared to DOC-1 (Fig. 4), the enhanced NO to N₂O conversion at low space velocity that was only observed over DOC-2 (Fig. 5b) may be explained by different particle sizes that could lead to different turnover frequencies (TOF) regarding hydrocarbon oxidation, NO to NO₂ oxidation, and NO to N₂O conversion. Based on the data shown in Fig. 5, one may speculate about different adsorption behavior over the two samples, i.e. by provision of more surface sites due to the higher loading of DOC-2 or by different adsorption energies and surface coverages as the consequence of variations of the particle size, morphology, and oxidation state [42,59–63]. Notably, also the various suggestions on the HC-SCR reaction mechanism and accompanying N₂O formation pathways that were proposed in literature may originate from slight differences of the catalyst state or morphology, which call for future fundamental studies with well-defined model catalysts exploiting bulk- and surface-sensitive *operando* characterization techniques. Hence, we renounce giving a final explanation for the different behavior on a microkinetic and microscopic level at this point and rather focus on the role of hydrocarbons on N₂O formation over the commercial oxidation catalysts in the following paragraph, which is of utmost importance in the light of real-world applications.

3.4. Influence of hydrocarbon

By replacing C₂H₄ by other hydrocarbons that can occur in the exhaust gas of lean-burn applications, namely C₂H₆, C₃H₆, and C₃H₈ as short-chain compounds and C₁₂H₂₆ as representative long-chain species, we evaluated their tendency to cause N₂O formation in the same temperature window and under identical operating conditions as described above. Notably, the species tested herein can be considered as potential reductant to reduce NO over noble metal catalysts, albeit with varying temperature regimes.

Simultaneous exposure of the catalysts to NO and either ethane (C₂H₆) or propane (C₃H₈) during a light-off up to 350 °C did not result in N₂O formation over either of the catalyst samples. In line with previous results that indicate an increasing reactivity with increasing chain length [64,65], C₂H₆ exhibits a higher stability than C₃H₈. While DOC-1 was unable to convert any of the C₂H₆, irrespective of the inlet concentration, and also DOC-2 shows only minimal C₂H₆ conversion even at 350 °C, DOC-1 and DOC-2 convert approx. 6% and 15% C₃H₈, respectively, in gas mix 3d at 350 °C and a space velocity of 60 000 h⁻¹ (cf. Figs. S5-S8). The overall higher activity for hydrocarbon conversion over DOC-2 can be attributed to its higher noble metal loading. While HC-SCR can be neglected in the investigated temperature regime, both catalysts oxidize NO to NO₂, showing the typical increase in the NO oxidation activity with rising temperature until the thermodynamic equilibrium benefits NO₂ decomposition to NO [10,53]. Although in the low-temperature regime neither C₂H₆ nor C₃H₈ are converted and also at elevated temperatures above 300 °C the conversion rates are very low, the inhibition of the NO to NO₂ oxidation is more pronounced when C₃H₈ is present in the gas stream. Hence, an actual conversion of the

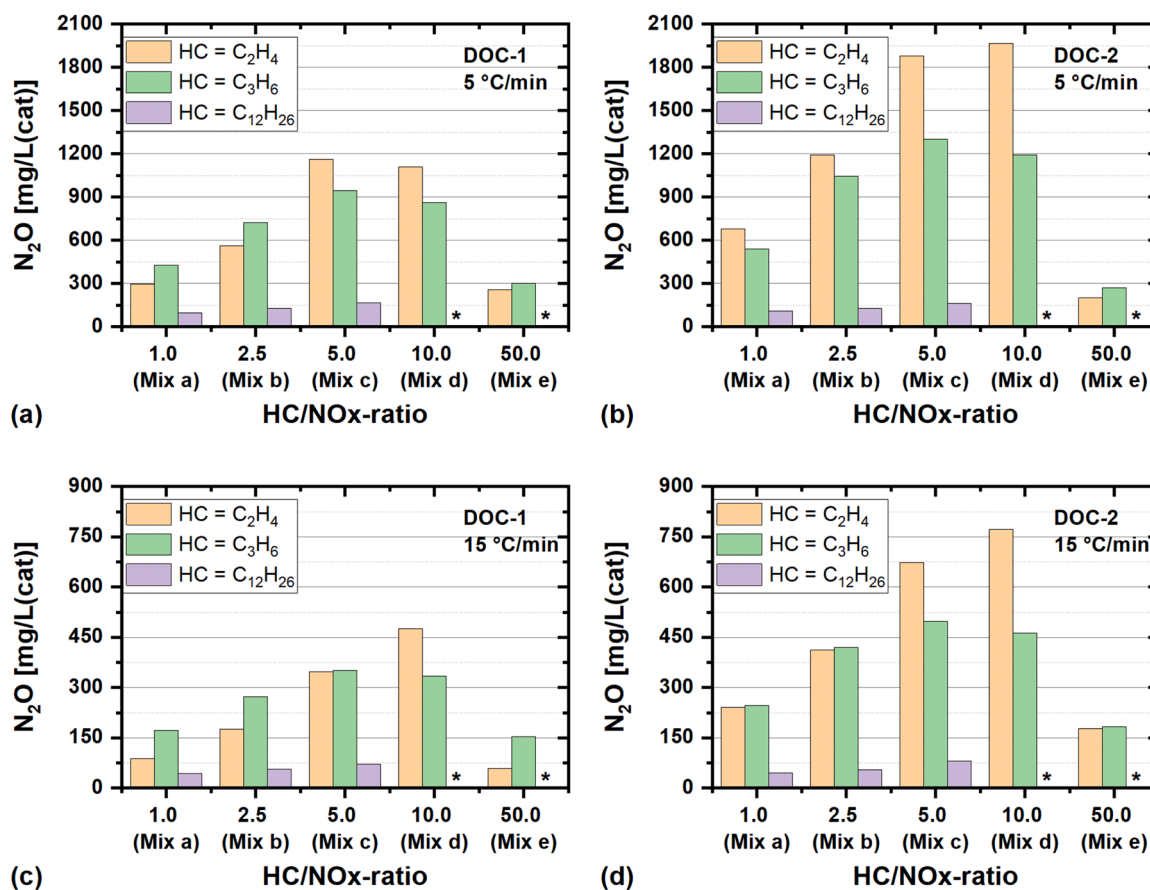


Fig. 6. Total amount of N₂O formed during a light-off from 150° to 350°C in 150 ppm NO, 150 – 7500 ppm HC (with HC = C₂H₄, C₃H₆, C₁₂H₂₆), 10 vol.-% O₂, 10 vol.-% H₂O, bal. N₂ (GHSV = 60 000 h⁻¹) over DOC-1 (a, c) and DOC-2 (b, d); ramp rate 5 °C/min (a, b) and 15 °C/min (c, d), respectively. *Mix d and e were not measured for the gas mix containing C₁₂H₂₆.

hydrocarbon does not seem to be a prerequisite for NO oxidation inhibition, but rather a mere adsorption and storage of the hydrocarbon can take place, which can efficiently block active surface sites that are then unavailable for NO adsorption and reaction.

Analogous to C₂H₄, also C₃H₆ formed significant amounts of N₂O during the light-off tests over a broad range of conditions (Fig. 6). N₂O formation presumably proceeds via the following global reaction Eq. (3):



This is a well-known phenomenon and has previously been reported as an undesired side-reaction during the selective catalytic reduction of NO using C₃H₆ as reductant [20,26,29,36].

Overall, the results discussed so far suggest that in the temperature window that is subject to this study, only the presence of unsaturated hydrocarbons gives rise to N₂O formation, whereas saturated hydrocarbons are hardly converted and therefore do not cause secondary emissions. However, our current results with C₁₂H₂₆ levels that are relevant in real-world applications suggest N₂O formation between 150 °C and 350 °C if NO and C₁₂H₂₆ interact on the Pt-Pd catalysts, similar to earlier results by Kamasamudram et al. [20] and despite the saturated nature of C₁₂H₂₆. Compared to the total amounts formed in the presence of C₂H₄ or C₃H₆, C₁₂H₂₆ yields substantially lower N₂O levels (Fig. 6). We assume that this behavior is due to the catalytic decomposition of C₁₂H₂₆. Earlier mechanistic investigations that typically combine experimental insights with kinetic models suggested that the conversion of C₁₂H₂₆ in the presence of O₂ takes place via the scission of longer HC-chains into HC-species with shorter chain length [66–70]. Subsequently, the reaction of unsaturated fragments that can occur among these short-chain species with NO results in formation of low N₂O levels. Exposure to gas mix 1b at a GHSV of 60 000 h⁻¹ and a ramp rate of 15 °C/min, for instance, results in a maximum N₂O concentration of approximately 4 ppm over both samples (Fig. S9). Although this is an almost negligible level compared to the tests with unsaturated hydrocarbons, the accumulated N₂O emissions over time are still relevant in the light of the enormous greenhouse potential of N₂O.

With regard to the total N₂O amounts formed when using either C₂H₄ or C₃H₆, not only the HC/NO_x ratio but also the noble metal loading and the ramp rate seem to strongly influence the N₂O formation. Over DOC-1, the interaction between NO and C₂H₄ results in significantly lower N₂O amounts than the NO-C₃H₆ interaction if a HC/NO_x ratio of 1.0 (mix a) or 2.5 (mix b) is chosen (Fig. 6a, c). In contrast, the evolving N₂O quantities become higher in gas mix c and d the presence of C₂H₄. With a HC/NO_x ratio of 50, this trend is reversing again and the NO-C₃H₆ interactions produce more N₂O. These trends are in line with the trends found when plotting the N₂O amount in relation to the NO amount dosed (Fig. S10). The behavior in mix e can be attributed to the earlier onset of the exothermicity effect when feeding the more reactive C₂H₄: During the light-off with 5 °C/min, full C₂H₄ conversion is observed already at an inlet temperature of 173 °C, which corresponds to an outlet temperature of 350 °C. On the other hand, C₃H₆ activation requires higher temperatures and lights-off rapidly above 205 °C (Fig. S11). Although the higher reactivity of C₂H₄ may also contribute to temperature profiles along the catalyst sample that benefit N₂O formation when using moderate HC/NO_x ratios, also chemical processes taking place on the catalyst surface can come into play. In their mechanistic investigation on HC-SCR utilizing the technique of temporal analysis of products (TAP), Burch et al. [34] pointed out that a single C₃H₆ molecule is capable of reacting with nine oxygen atoms that are adsorbed on the platinum surface. Since reduced platinum sites are considered a prerequisite for nitrogen oxide adsorption, the affinity of the hydrocarbon towards oxidation is of utmost importance. Considering the higher reactivity of C₂H₄, we can speculate about a faster consumption of adsorbed oxygen atoms that are then available for NO adsorption and subsequent partial reduction to N₂O. With respect to the surface oxygen concentration, however, the impact of the HC reactivity

could be less important at low hydrocarbon concentrations and moderate catalytic activity for oxidation reactions. Instead, the maximum number of consumed O atoms per HC molecule – 9 for C₃H₆ versus 6 for C₂H₄ – may dominate the surface species coverage. Such an overall more efficient consumption of oxygen atoms over DOC-2 would not only explain the overall higher N₂O levels over DOC-2, but would also explain the different behavior of DOC-1 and DOC-2 in gas mix a and b. While DOC-2 with its high noble metal loading sufficiently catalyzes the hydrocarbon oxidation also at low concentrations, the removal of O surface atoms is less efficient over the less active DOC-1, possibly due to the lower local heat evolution as a result of less efficient exothermic hydrocarbon oxidation.

In addition to the overall N₂O amount formed during light-off, the influence of the HC/NO_x ratio that was already extensively discussed for C₂H₄ (cf. Section 3.2) seems to change when using C₃H₆ as reductant instead. As illustrated in Fig. 7, an increasing C₃H₆ concentration does not only go along with an increasing maximum N₂O concentration, but the maximum N₂O value is shifted towards higher temperatures for higher C₃H₆ inlet concentrations. While these observations are in line with earlier results reported by Acke et al. [29], who investigated NO_x reduction with propene over Pt/ZSM-5 catalysts, the trends observed when using C₃H₆ are clearly inverted compared to the trends observed for the kinetic tests with C₂H₄ (Fig. 2c, d). Since the temperature $T(c(N_2O)_{max})$ reported herein always represents the inlet temperature that is measured approx. 2 mm upstream the catalyst sample, we do not assume a bias of the temperature data due to a different exothermicity of the hydrocarbon oxidation reactions. Hence, the reason for this difference is most likely of a mechanistic nature. As the hydrocarbon surface coverage is assumed to govern HC-deNO_x and the accompanying N₂O formation [29], one may speculate about a different adsorption behavior of C₂H₄ and C₃H₆ and consequently different surface coverages with hydrocarbon species that compete with oxygen and NO for surface sites [64,71]. In particular, Acke et al. [29] assumed the formation of an inactive surface layer with C₃H₆ species, which may explain the shift of $T(c(N_2O)_{max})$ towards higher temperatures when increasing the C₃H₆ inlet concentration. Also, differences in the power of the reducing agent are of high relevance as reported by Burch et al. [34], since the ability of the reductant to react with adsorbed oxygen atoms ensures the availability of a reduced platinum surface for NO adsorption and reaction. With respect to HC-SCR regimes and NO to NO₂ oxidation when C₃H₆ is fed (Fig. S12), we found an analogous behavior to C₂H₄, even if the temperature regimes that benefit either of the two processes are slightly shifted compared to the gas composition containing C₂H₄. These results confirm earlier results in the context of C₃H₆-NO-interactions in excess oxygen that point to an inhibition of NO oxidation over platinum-based oxidation catalysts in the presence of C₃H₆ [49].

Future fundamental studies with a focus on mechanistic insights are highly desirable for uncovering the origin of the different behavior of C₂H₄ and C₃H₆ in detail and may additionally clarify the exact N₂O formation pathway that is still under debate. However, even without final mechanistic insights on a microkinetic level, our current data under conditions relevant for real-world applications clearly demonstrate that the type of hydrocarbon is one of the key parameters governing N₂O formation from NO over noble metal catalysts. When designing operation modes and exhaust tailpipes for lean-burn combustion engines that aim at avoiding N₂O evolution, these findings need to be considered.

4. Conclusions

In view of the growing awareness of secondary emissions evolving from modern catalytic converters for emission control, this study investigates the formation of N₂O over Pt-Pd oxidation catalysts as a consequence of interactions between hydrocarbons and NO. In a series of kinetic light-off tests between 150 °C and 350 °C under conditions relevant for lean-burn engines, the interaction of NO with the unsaturated hydrocarbons C₂H₄ and C₃H₆ resulted in pronounced formation of

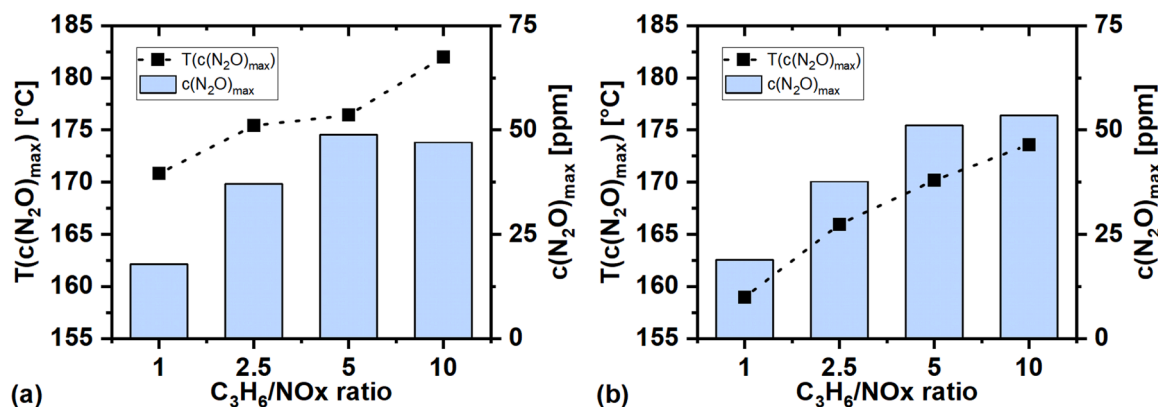


Fig. 7. Maximum N₂O concentration with the corresponding temperature for (a) DOC-1 and (b) DOC-2 during a light-off in 150 ppm NO, 150 – 7500 ppm C₃H₆, 10 vol.-% O₂, 10 vol.-% H₂O, bal. N₂ (5 °C/min, GHSV = 60 000 h⁻¹).

N₂O even beyond the point of their full conversion. Herein, N₂O is the outcome of an undesired side reaction of the selective catalytic reduction of NO using hydrocarbons (HC-SCR). In contrast, the saturated hydrocarbons C₂H₆ and C₃H₈ were barely converted below 350 °C, hence, no N₂O was formed. C₁₂H₂₆ gave rise to small N₂O quantities, which we attribute to the C₁₂H₂₆ decomposition mechanism via chain-splitting and involvement of unsaturated short-chain fragments. Variations of the HC/NO_x ratio suggest an increasing N₂O formation with increasing HC-content, which can be attributed to an efficient removal of surface oxygen atoms from the noble metal, hereby creating free surface sites for the adsorption and conversion of NO. Once the exothermicity of the hydrocarbon oxidation is capable of heating the catalyst beyond the critical low-temperature regime that benefits N₂O formation, N₂O formation drops. For instance, a HC/NO_x ratio of 50 results in significantly lower N₂O formation than a HC/NO_x ratio of 10. Passing through the critical low-temperature window as fast as possible, i.e. by faster heating, was identified as most effective measure to reduce N₂O formation. In terms of real-world applications, a fast temperature increase above the critical temperature range regarding N₂O formation, e.g. by electrical heating of catalytic converters, could be a feasible option. In addition, the presence of very high hydrocarbon concentrations that are oxidized over the catalyst and cause significant heat evolution could be exploited, since the pronounced exothermicity can sufficiently heat the catalyst to skip the critical temperature range in which N₂O formation can occur.

Moreover, the hydrocarbon concentration and the reactivity of the hydrocarbon have an impact on the oxidation of NO to NO₂. When using C₂H₄ as reductant, for instance, the HC-SCR reaction regime dominates up to approximately 250 °C and is followed by a temperature regime above 300 °C that is dominated by NO oxidation. While rising HC concentrations promote NO conversion – mainly due to undesired reduction to N₂O – hydrocarbons inhibit NO oxidation to NO₂, which needs to be considered when designing a modern and highly efficient overall exhaust tailpipe. In summary, these results underscore that already minor variations in the reaction conditions can tremendously change the dominant reaction mechanism and the corresponding product species concentrations. In addition, a higher noble metal loading facilitates hydrocarbon activation at low temperatures, governs an earlier onset of exothermicity, and corresponds to increasing N₂O amounts formed during the light-off test.

From a fundamental point of view, the roles of the noble metal particle size, alloying, and oxidation state that were beyond the scope of our present study deserve to be investigated in more detail during future studies focusing on surface and bulk phenomena, possibly supplemented by microkinetic modeling that can help to understand the complex interactions between NO_x and hydrocarbons. With regard to industrial relevance, an increasing use of biofuels and synthetic fuels produced

from renewable feedstocks that exhibit a different molecular composition compared to conventional fuels can require adaptations regarding the combustion technology [72]. Ultimately, such changes could make the prevention of secondary emission evolution in the exhaust tailpipe even more important. Hence, comprehensive considerations taking the fuel and the combustion technology into account are not only a prerequisite for developing novel catalyst materials with high activity and selectivity for future applications, but can also help refining operation procedures in real-world applications. On the long run, this scenario may call for further measures to mitigate N₂O formation, for instance by fast external heating.

CRediT authorship contribution statement

Patrick Lott: Conceptualization, Methodology, Validation, Formal analysis, Investigation, Resources, Data curation, Writing – original draft, Visualization, Project administration. **Simon Bastian:** Investigation. **Heike Többen:** Conceptualization, Methodology, Resources, Writing – review & editing. **Lisa Zimmermann:** Validation, Writing – review & editing. **Olaf Deutschmann:** Resources, Writing – review & editing, Project administration.

Declaration of Competing Interest

The authors declare that they have no known competing financial interests or personal relationships that could have appeared to influence the work reported in this paper.

Data Availability

Data will be made available on request.

Acknowledgement

The authors thank the Helmholtz program “Materials and Technologies for the Energy Transition” (MTET) and chemogy GmbH for financial support.

Appendix A. Supporting information

Supplementary data associated with this article can be found in the online version at [doi:10.1016/j.apcata.2023.119028](https://doi.org/10.1016/j.apcata.2023.119028).

References

- [1] M.V. Twigg, Catalytic control of emissions from cars, *Catal. Today* 163 (2011) 33–41, <https://doi.org/10.1016/j.cattod.2010.12.044>.

- [2] O. Deutschmann, J.-D. Grunwaldt, Exhaust gas aftertreatment in mobile systems: status, challenges, and perspectives, *Chem. Ing. Tech.* 85 (2013) 595–617, <https://doi.org/10.1002/cite.201200188>.
- [3] R.J. Farrauto, M. Deeba, S. Alerasool, Gasoline automobile catalysis and its historical journey to cleaner air, *Nat. Catal.* 2 (2019) 603–613, <https://doi.org/10.1038/s41929-019-0312-9>.
- [4] P. Lott, O. Deutschmann, Lean-burn natural gas engines: challenges and concepts for an efficient exhaust gas aftertreatment system, *Emiss. Control Sci. Technol.* 7 (2021) 1–6, <https://doi.org/10.1007/s40825-020-00176-w>.
- [5] P. Nevalainen, N.M. Kinnunen, A. Kirveslahti, K. Kallinen, T. Maunula, M. Keenan, M. Suvanto, Formation of NH_3 and N_2O in a modern natural gas three-way catalyst designed for heavy-duty vehicles: the effects of simulated exhaust gas composition and ageing, *Appl. Catal. A* 552 (2018) 30–37, <https://doi.org/10.1016/j.apcata.2017.12.017>.
- [6] C.X. Wang, J.W. Tan, G. Harle, H.M. Gong, W.Z. Xia, T.T. Zheng, D.X. Yang, Y. S. Ge, Y.K. Zhao, Ammonia formation over Pd/Rh three-way catalysts during lean-to-rich fluctuations: the effect of the catalyst aging, exhaust temperature, lambda, and duration in rich conditions, *Environ. Sci. Technol.* 53 (2019) 12621–12628, <https://doi.org/10.1021/acs.est.9b03893>.
- [7] W.B. Bae, D.Y. Kim, S.W. Byun, M. Hazlett, D.Y. Yoon, C. Jung, C.H. Kim, S. B. Kang, Emission of NH_3 and N_2O during NO reduction over commercial aged three-way catalyst (TWC): Role of individual reductants in simulated exhausts, *Chem. Eng. J. Adv.* 9 (2022), 100222, <https://doi.org/10.1016/j.cej.2021.100222>.
- [8] J. Han, A.Y. Wang, G. Isapour, H. Härelind, M. Skoglundh, D. Creaser, L. Olsson, N_2O formation during NH_3 -SCR over different zeolite frameworks: effect of framework structure, copper species, and water, *Ind. Eng. Chem. Res.* 60 (2021) 17826–17839, <https://doi.org/10.1021/acs.iecr.1c02732>.
- [9] Y.X. Feng, T.V.W. Janssens, P.N.R. Venestrom, J. Jansson, M. Skoglundh, H. Grönbeck, The role of H^+ - and Cu^+ -sites for N_2O formation during NH_3 -SCR over Cu-CHA, *J. Phys. Chem. C* 125 (2021) 4595–4601, <https://doi.org/10.1021/acs.jpcc.0c11008>.
- [10] M. Borchers, K. Keller, P. Lott, O. Deutschmann, Selective catalytic reduction of NO_x with H_2 for cleaning exhausts of hydrogen engines: impact of H_2O , O_2 , and NO/H_2 ratio, *Ind. Eng. Chem. Res.* 60 (2021) 6613–6626, <https://doi.org/10.1021/acs.iecr.0c05630>.
- [11] D. Zengel, P. Koch, B. Torkashvand, J.-D. Grunwaldt, M. Casapu, O. Deutschmann, Emission of toxic HCN During NO_x removal by ammonia SCR in the exhaust of lean-burn natural gas engines, *Angew. Chem., Int. Ed.* 59 (2020) 14423–14428, <https://doi.org/10.1002/anie.202003670>.
- [12] A.B. Ngo, T.H. Vuong, H. Atia, U. Bentrup, V.A. Kondratenko, E.V. Kondratenko, J. Rabeah, U. Ambruster, A. Brückner, Effect of formaldehyde in selective catalytic reduction of NO_x by ammonia (NH_3 -SCR) on a commercial V_2O_5 - WO_3 - TiO_2 catalyst under model conditions, *Environ. Sci. Technol.* 54 (2020) 11753–11761, <https://doi.org/10.1021/acs.est.0c00884>.
- [13] M. Elsener, R.J.G. Nuguid, O. Kröcher, D. Ferri, HCN production from formaldehyde during the selective catalytic reduction of NO_x with NH_3 over V_2O_5 / WO_3 - TiO_2 , *Appl. Catal. B* 281 (2021), 119462, <https://doi.org/10.1016/j.apcatb.2020.119462>.
- [14] M. Jablonska, R. Palkovits, It is no laughing matter: nitrous oxide formation in diesel engines and advances in its abatement over rhodium-based catalysts, *Catal. Sci. Technol.* 6 (2016) 7671–7687, <https://doi.org/10.1039/c6cy01126h>.
- [15] R.L. Thompson, L. Lassaletta, P.K. Patra, C. Wilson, K.C. Wells, A. Gressent, E. N. Koffi, M.P. Chipperfield, W. Winiwarter, E.A. Davidson, H. Tian, J.G. Canadell, Acceleration of global N_2O emissions seen from two decades of atmospheric inversion, *Nat. Clim. Change* 9 (2019) 993–998, <https://doi.org/10.1038/s41558-019-0613-7>.
- [16] S.K. Hoekman, Review of nitrous oxide (N_2O) emissions from motor vehicles, *SAE Int. J. Fuels Lubr.* 13 (2020) 79–98, <https://doi.org/10.4271/04-13-01-0005>.
- [17] E. Behrentz, R. Ling, P. Rieger, A.M. Winer, Measurements of nitrous oxide emissions from light-duty motor vehicles: a pilot study, *Atmos. Environ.* 38 (2004) 4291–4303, <https://doi.org/10.1016/j.atmosenv.2004.04.027>.
- [18] I. Mejía-Centeno, A. Martínez-Hernández, G.A. Fuentes, Effect of low-sulfur fuels upon NH_3 and N_2O emission during operation of commercial three-way catalytic converters, *Top. Catal.*, 42–43 (2007) 381–385, <https://doi.org/10.1007/s11244-007-0210-2>.
- [19] R. Wunsch, C. Schön, M. Frey, D. Tran, S. Proskes, T. Wandrey, M. Kalogirou, J. Schäffner, Detailed experimental investigation of the NO_x reaction pathways of three-way catalysts with focus on intermediate reactions of NH_3 and N_2O , *Appl. Catal. B* 272 (2020), <https://doi.org/10.1016/j.apcatb.2020.118937>.
- [20] K. Kamasamudram, C. Henry, N. Currier, A. Yezerets, N_2O formation and mitigation in diesel aftertreatment systems, *SAE Int. J. Engines* 5 (2012) 688–698, <https://doi.org/10.4271/2012-01-1085>.
- [21] M. Yates, J.A. Martin, M.A. Martin-Luengo, S. Suarez, J. Blanco, N_2O formation in the ammonia oxidation and in the SCR process with V_2O_5 - WO_3 catalysts, *Catal. Today* 107 (8) (2005) 120–125, <https://doi.org/10.1016/j.cattod.2005.07.015>.
- [22] M.H. Zhu, J.K. Lai, I.E. Wachs, Formation of N_2O greenhouse gas during SCR of NO with NH_3 by supported vanadium oxide catalysts, *Appl. Catal. B* 224 (2018) 836–840, <https://doi.org/10.1016/j.apcatb.2017.11.029>.
- [23] D. Zhang, R.T. Yang, N_2O formation pathways over zeolite-supported Cu and Fe catalysts in NH_3 -SCR, *Energy Fuels* 32 (2018) 2170–2182, <https://doi.org/10.1021/acs.energyfuels.7b03405>.
- [24] R. Burch, P.J. Millington, Selective reduction of nitrogen-oxides by hydrocarbons under lean-burn conditions using supported platinum group metal catalysts, *Catal. Today* 26 (1995) 185–206, [https://doi.org/10.1016/0920-5861\(95\)00136-4](https://doi.org/10.1016/0920-5861(95)00136-4).
- [25] R. Burch, J.P. Breen, F.C. Meunier, A review of the selective reduction of NO_x with hydrocarbons under lean-burn conditions with non-zeolitic oxide and platinum group metal catalysts, *Appl. Catal. B* 39 (2002) 283–303, [https://doi.org/10.1016/S0926-3373\(02\)00118-2](https://doi.org/10.1016/S0926-3373(02)00118-2).
- [26] M. Khosravi, C. Sola, A. Abedi, R.E. Hayes, W.S. Epling, M. Votsmeier, Oxidation and selective catalytic reduction of NO by propene over Pt and Pt/Pd diesel oxidation catalysts, *Appl. Catal. B* 147 (2014) 264–274, <https://doi.org/10.1016/j.apcatb.2013.08.034>.
- [27] G.R. Bamwenda, A. Obuchi, A. Ogata, K. Mizuno, An FTIR study of the species adsorbed on a Rh/ Al_2O_3 catalyst in the selective reduction of NO by propylene, *Chem. Lett.* (1994) 2109–2112, <https://doi.org/10.1246/cl.1994.2109>.
- [28] D.I. Kondarides, T. Chafik, X.E. Verykios, Catalytic reduction of NO by CO over rhodium catalysts. 3. The role of surface isocyanate species, *J. Catal.* 193 (2000) 303–307, <https://doi.org/10.1006/jcat.2000.2892>.
- [29] F. Acke, M. Skoglundh, Zeolite supported Pt catalysts for reduction of NO under oxygen excess: a comparison of C_3H_6 , HNCO and NH_3 as reducing agents, *Appl. Catal. B* 20 (1999) 235–242, [https://doi.org/10.1016/S0926-3373\(98\)00114-3](https://doi.org/10.1016/S0926-3373(98)00114-3).
- [30] T. Tanaka, T. Okuhara, M. Misono, Intermediacy of organic nitro and nitrite surface species in selective reduction of nitrogen monoxide by propene in the presence of excess oxygen over silica-supported platinum, *Appl. Catal. B* 4 (1994) L1–L9, [https://doi.org/10.1016/0926-3373\(94\)00015-8](https://doi.org/10.1016/0926-3373(94)00015-8).
- [31] M. Haneda, E. Joubert, J.C. Menezes, D. Duprez, J. Barbier, N. Bion, M. Daturi, J. Saussey, J.C. Lavalley, H. Hamada, Reaction intermediates in the selective reduction of NO with propene over Ga_2O_3 - Al_2O_3 and In_2O_3 - Al_2O_3 catalysts, *J. Mol. Catal. A* 175 (2001) 179–188, [https://doi.org/10.1016/S1381-1169\(01\)00215-1](https://doi.org/10.1016/S1381-1169(01)00215-1).
- [32] E. Joubert, J.C. Menezes, D. Duprez, J. Barbier, GC-MS identification of organic by-products of the NO SCR by propene; relation to N_2O formation, *Top. Catal.* 16 (2001) 225–229, <https://doi.org/10.1023/A:1016628108404>.
- [33] E. Joubert, X. Courtois, P. Marecot, C. Canaff, D. Duprez, The chemistry of DeNOx reactions over Pt/ Al_2O_3 : the oxime route to N_2 or N_2O , *J. Catal.* 243 (2006) 252–262, <https://doi.org/10.1016/j.jcat.2006.07.018>.
- [34] R. Burch, P.J. Millington, A.P. Walker, Mechanism of the selective reduction of nitrogen monoxide on platinum-based catalysts in the presence of excess oxygen, *Appl. Catal. B* 4 (1994) 65–94, [https://doi.org/10.1016/0926-3373\(94\)00014-X](https://doi.org/10.1016/0926-3373(94)00014-X).
- [35] B.K. Cho, J.E. Yie, Nitric oxide reduction by ethylene over Pt-ZSM-5 under lean conditions: steady-state activity, *Appl. Catal. B* 10 (1996) 263–280, [https://doi.org/10.1016/S0926-3373\(96\)00002-1](https://doi.org/10.1016/S0926-3373(96)00002-1).
- [36] R. Burch, J.A. Sullivan, T.C. Watling, Mechanistic considerations for the reduction of NO_x over Pt/ Al_2O_3 and Al_2O_3 catalysts under lean-burn conditions, *Catal. Today* 42 (1998) 13–23, [https://doi.org/10.1016/S0920-5861\(98\)00072-8](https://doi.org/10.1016/S0920-5861(98)00072-8).
- [37] B.K. Cho, Elucidation of Lean- NO_x reduction mechanism using kinetic isotope effect, *J. Catal.* 178 (1998) 395–407, <https://doi.org/10.1006/jcat.1998.2169>.
- [38] N.W. Cant, D.E. Angove, D.C. Chambers, Nitrous oxide formation during the reaction of simulated exhaust streams over rhodium, platinum and palladium catalysts, *Appl. Catal. B* 17 (1998) 63–73, [https://doi.org/10.1016/S0926-3373\(97\)00105-7](https://doi.org/10.1016/S0926-3373(97)00105-7).
- [39] P. Denton, A. Giroir-Fendler, H. Pralraud, M. Primet, Role of the nature of the support (alumina or silica), of the support porosity, and of the Pt dispersion in the selective reduction of NO by C_3H_6 under lean-burn conditions, *J. Catal.* 189 (2000) 410–420, <https://doi.org/10.1006/jcat.1999.2708>.
- [40] R. Burch, T.C. Watling, The difference between alkanes and alkenes in the reduction of NO by hydrocarbons over Pt catalysts under lean-burn conditions, *Catal. Lett.* 43 (1997) 19–23, <https://doi.org/10.1023/A:1018974102756>.
- [41] T.W. Hansen, A.T. Delariva, S.R. Challa, A.K. Datye, Sintering of catalytic nanoparticles: particle migration or Ostwald ripening, *Acc. Chem. Res.* 46 (2013) 1720–1730, <https://doi.org/10.1021/ar3002427>.
- [42] J. Schütz, H. Störmer, P. Lott, O. Deutschmann, Effects of hydrothermal aging on CO and NO oxidation activity over monometallic and bimetallic Pt-Pd catalysts, *Catalysts* 11 (2021) 300, <https://doi.org/10.3390/catal11030300>.
- [43] P. Lott, M. Eck, D.E. Doronkin, R. Popescu, M. Casapu, J.-D. Grunwaldt, O. Deutschmann, Regeneration of sulfur poisoned Pd-Pt/ CeO_2 - ZrO_2 - Y_2O_3 - La_2O_3 and Pd-Pt/ Al_2O_3 methane oxidation catalysts, *Top. Catal.* 62 (2019) 164–171, <https://doi.org/10.1007/s11244-018-1121-0>.
- [44] S.C. Shen, S. Kawi, Selective catalytic reduction of NO by hydrocarbons in the presence of excess oxygen using Pt/MCM-41 catalysts, *Appl. Catal. B* 45 (2003) 63–76, [https://doi.org/10.1016/S0926-3373\(03\)00108-5](https://doi.org/10.1016/S0926-3373(03)00108-5).
- [45] R. Burch, P. Fornasiero, T.C. Watling, Kinetics and mechanism of the reduction of NO by n-octane over Pt/ Al_2O_3 under lean-burn conditions, *J. Catal.* 176 (1998) 204–214, <https://doi.org/10.1006/jcat.1998.2024>.
- [46] R. Burch, D. Ottery, Selective catalytic reduction of NO_x by hydrocarbons on Pt/ Al_2O_3 catalysts at low temperatures without the formation of N_2O , *Appl. Catal. B* 9 (1996) L19–L24, [https://doi.org/10.1016/0926-3373\(96\)90071-5](https://doi.org/10.1016/0926-3373(96)90071-5).
- [47] A. Obuchi, A. Ogata, H. Takahashi, J. Oi, G.R. Bamwenda, K. Mizuno, Selective reduction of nitrogen oxides with various organic substances on precious metal catalysts under a high GHSV condition, *Catal. Today* 29 (1996) 103–107, [https://doi.org/10.1016/0920-5861\(95\)00287-1](https://doi.org/10.1016/0920-5861(95)00287-1).
- [48] C. Rottländer, R. Andorf, C. Plog, B. Krutzsch, M. Baerns, Selective NO reduction by propane and propene over a Pt/ZSM-5 catalyst: a transient study of the reaction mechanism, *Appl. Catal. B* 11 (1996) 49–63, [https://doi.org/10.1016/S0926-3373\(96\)00038-0](https://doi.org/10.1016/S0926-3373(96)00038-0).
- [49] K. Irani, W.S. Epling, R. Blint, Effect of hydrocarbon species on no oxidation over diesel oxidation catalysts, *Appl. Catal. B* 92 (2009) 422–428, <https://doi.org/10.1016/j.apcatb.2009.08.022>.
- [50] C. Henry, N. Currier, N. Ottinger, A. Yezerets, M. Castagnola, H.-Y. Chen, H. Hess, Decoupling the Interactions of Hydrocarbons and Oxides of Nitrogen Over Diesel Oxidation Catalysts, *SAE International*, 2011.

- [51] L. Olsson, E. Fridell, The influence of Pt oxide formation and Pt dispersion on the reactions $\text{NO}_2 \rightleftharpoons \text{NO} + 1/2 \text{O}_2$ over Pt/Al₂O₃ and Pt/BaO/Al₂O₃, *J. Catal.* 210 (2002) 340–353, <https://doi.org/10.1006/jcat.2002.3698>.
- [52] E. Ogel, M. Casapu, D.E. Doronkin, R. Popescu, H. Störmer, C. Mechler, G. Marzun, S. Barcikowski, M. Türk, J.-D. Grunwaldt, Impact of preparation method and hydrothermal aging on particle size distribution of Pt/ γ -Al₂O₃ and its performance in CO and NO oxidation, *J. Phys. Chem. C* 123 (2019) 5433–5446, <https://doi.org/10.1021/acs.jpcc.8b11065>.
- [53] M. Crocoll, S. Kureti, W. Weisweiler, Mean field modeling of NO oxidation over Pt/Al₂O₃ catalyst under oxygen-rich conditions, *J. Catal.* 229 (2005) 480–489, <https://doi.org/10.1016/j.jcat.2004.11.029>.
- [54] P. Lott, P. Dolcet, M. Casapu, J.-D. Grunwaldt, O. Deutschmann, The effect of prereduction on the performance of Pd/Al₂O₃ and Pd/CeO₂ catalysts during methane oxidation, *Ind. Eng. Chem. Res.* 58 (2019) 12561–12570, <https://doi.org/10.1021/acs.iecr.9b01267>.
- [55] W.S. Epling, L.E. Campbell, A. Yezerets, N.W. Currier, J.E. Parks, Overview of the fundamental reactions and degradation mechanisms of NO_x storage/reduction catalysts, *Catal. Rev.* 46 (2004) 163–245, <https://doi.org/10.1081/Cr-200031932>.
- [56] J.H. Lee, H.H. Kung, Effect of Pt dispersion on the reduction of NO by propene over alumina-supported Pt catalysts under lean-burn conditions, *Catal. Lett.* 51 (1998) 1–4, <https://doi.org/10.1023/A:1019068530266>.
- [57] E. Seker, E. Gulari, Improved N₂ selectivity for platinum on alumina prepared by sol-gel technique in the reduction of NO_x by propene, *J. Catal.* 179 (1998) 339–342, <https://doi.org/10.1006/jcat.1998.2246>.
- [58] E. Seker, E. Gulari, Activity and N₂ selectivity of sol-gel prepared Pt/alumina catalysts for selective NO_x reduction, *J. Catal.* 194 (2000) 4–13, <https://doi.org/10.1006/jcat.2000.2949>.
- [59] K. Hauff, H. Dubbe, U. Tuttlies, G. Eigenberger, U. Nieken, Platinum oxide formation and reduction during NO oxidation on a diesel oxidation catalyst-Macrokinetic simulation, *Appl. Catal. B* 129 (2013) 273–281, <https://doi.org/10.1016/j.apcatb.2012.09.022>.
- [60] D. Chan, S. Tischer, J. Heck, C. Diehm, O. Deutschmann, Correlation between catalytic activity and catalytic surface area of a Pt/Al₂O₃ DOC: An experimental and microkinetic modeling study, *Appl. Catal. B* 156 (2014) 153–165, <https://doi.org/10.1016/j.apcatb.2014.03.009>.
- [61] X. Auvray, L. Olsson, Stability and activity of Pd-, Pt- and Pd-Pt catalysts supported on alumina for NO oxidation, *Appl. Catal. B* 168 (2015) 342–352, <https://doi.org/10.1016/j.apcatb.2014.12.035>.
- [62] T.K. Hansen, M. Hoj, B.B. Hansen, T.V.W. Janssens, A.D. Jensen, The effect of Pt particle size on the oxidation of CO, C₃H₆, and NO over Pt/Al₂O₃ for diesel exhaust aftertreatment, *Top. Catal.* 60 (2017) 1333–1344, <https://doi.org/10.1007/s11244-017-0818-9>.
- [63] F. Maurer, A. Gänzler, P. Lott, B. Betz, M. Votsmeier, S. Loridant, P. Vernoux, V. Murzin, B. Bornmann, R. Frahm, O. Deutschmann, M. Casapu, J.-D. Grunwaldt, Spatiotemporal investigation of the temperature and structure of a Pt/CeO₂ oxidation catalyst for CO and hydrocarbon oxidation during pulse activation, *Ind. Eng. Chem. Res.* 60 (2021) 6662–6675, <https://doi.org/10.1021/acs.iecr.0c05798>.
- [64] G. Veser, L.D. Schmidt, Ignition and extinction in the catalytic oxidation of hydrocarbons over platinum, *AIChE J.* 42 (1996) 1077–1087, <https://doi.org/10.1002/aic.690420418>.
- [65] M. Aryafar, F. Zaera, Kinetic study of the catalytic oxidation of alkanes over nickel, palladium, and platinum foils, *Catal. Lett.* 48 (1997) 173–183, <https://doi.org/10.1023/A:1019055810760>.
- [66] E. Ranzi, A. Frassoldati, S. Granata, T. Faravelli, Wide-range kinetic modeling study of the pyrolysis, partial oxidation, and combustion of heavy n-alkanes, *Ind. Eng. Chem. Res.* 44 (2005) 5170–5183, <https://doi.org/10.1021/ie049318g>.
- [67] C.K. Westbrook, W.J. Pitz, O. Herbinet, H.J. Curran, E.J. Silke, A comprehensive detailed chemical kinetic reaction mechanism for combustion of n-alkane hydrocarbons from n-octane to n-hexadecane, *Combust. Flame* 156 (2009) 181–199, <https://doi.org/10.1016/j.combustflame.2008.07.014>.
- [68] M.S. Kurman, R.H. Natelson, N.P. Cernansky, D.L. Miller, Speciation of the reaction intermediates from n-dodecane oxidation in the low temperature regime, *Proc. Combust. Inst.* 33 (2011) 159–166, <https://doi.org/10.1016/j.proci.2010.05.038>.
- [69] K. Narayanaswamy, P. Pepiot, H. Pitsch, A chemical mechanism for low to high temperature oxidation of n-dodecane as a component of transportation fuel surrogates, *Combust. Flame* 161 (2014) 866–884, <https://doi.org/10.1016/j.combustflame.2013.10.012>.
- [70] R.K. Dadi, R. Daya, G.K. Reddy, A. Kumar, A. Srinivasan, H.M. An, M. J. Cunningham, S.Y. Joshi, N.W. Currier, A. Yezerets, Modeling and experimental insights on oxidation of heavy chain HCs on diesel oxidation catalysts, *Chem. Eng. J.* 435 (2022) 134996, <https://doi.org/10.1016/j.cej.2022.134996>.
- [71] I.V. Yentekakis, V. Tellou, G. Botzoulaki, I.A. Rapakousios, A comparative study of the C₃H₆ + NO + O₂, C₃H₆ + O₂ and NO + O₂ reactions in excess oxygen over Na-modified Pt/ γ -Al₂O₃ catalysts, *Appl. Catal. B* 56 (2005) 229–239, <https://doi.org/10.1016/j.apcatb.2004.08.017>.
- [72] W. Leitner, J. Klankermayer, S. Pischinger, H. Pitsch, K. Kohse-Höinghaus, Advanced biofuels and beyond: chemistry solutions for propulsion and production, *Angew. Chem., Int. Ed.* 56 (2017) 5412–5452, <https://doi.org/10.1002/anie.201607257>.